

Majorana Neutrino Mass Matrices with a Texture Zero and a Cofactor Zero under Current Experimental Texts

Wei Jian Wang^{1,2} and Dong-Jiang Zhang³

¹*Department of Physics, North China Electric Power University, Baoding 071003, P. R. China*

²*Zhejiang Institute of Modern Physics, Zhejiang University, Hangzhou 310027, P.R. China**

³*Department of Physics, Zhejiang University, Hangzhou, P.R. China*

Abstract

The Majorana neutrino mass textures with a texture zero and a vanishing cofactor are re-considered in the light of current experimental results. A numerical and systematic analysis is carried out for all viable patterns. In particular, we focus on the phenomenological implication of correlations between three mixing angle (especially for θ_{23}), Dirac CP-violating phase δ , the effective Majorana neutrino mass m_{ee} . We demonstrated that the correlations between these variables play an important role in the model selection and can be measured in future long-baseline oscillation and neutrinoless double beta decay. Among the six viable patterns, it is the type-III with normal hierarchy and type-VI with inverted hierarchy that have the parameter space where the atmospheric neutrino mixing angle θ_{23} is less than maximal and the Dirac CP-violating phase covers its best-fit value.

Keywords: Majorana neutrino mass matrix, texture zero and cofactor zero, current experimental text.

*Electronic address: wjnwang96@gmail.com

By this time, various neutrino oscillation experiments have provided us with convincing evidences for massive neutrinos and leptonic flavor mixing with high degree of accuracy[1–3]. The large reactor angle $\theta_{13}(\approx 9^\circ)$ opens the door for us to explore the leptonic Dirac-CP violation and the mass hierarchy in the future long-baseline oscillation experiments. The absolute neutrino mass scale are strongly constrained by the cosmology observation[4, 5] and neutrinoless double-beta decay ($0\nu\beta\beta$) experiments (for a review, see [6]). On the other hand, it is still the main theoretical challenge to understand dynamic origin behind the observed bi-large structure of leptonic flavor mixing and the mass hierarchy spectrum. Although a full theory is still missing, several flavor symmetries have been proposed within the seesaw mechanism to reduce the number of free parameters in Yukawa sector and reveal the phenomenologically acceptable mixing pattern. These ideas include texture zeros[8], hybrid textures[9, 10], zero trace[11], zero determinant[12], vanishing minors[13, 14], two traceless submatrices[15], equal elements or cofactors[16], hybrid M_ν^{-1} textures[17]. Among these models, the textures with zero elements or zero minors are particularly appealed, which is not only because the textures can be naturally realized by introducing proper flavor symmetry, but also they are stable against the one-loop quantum corrections as the running of RGEs from seesaw scale Λ to the electroweak scale $\mu \simeq M_Z$.

In this work, we reconsider the Majorana neutrino mass textures with one texture and one vanishing minor, which have been studied in Ref.[14]. These models can be realized by $Z_{12} \times Z_2$ flavor symmetry. There are six types of textures compatible with the neutrino oscillation data. Our aim is to perform a more updated and complete analysis on these texture based on the current experimental data including the large reactor angle and the new cosmological bound on the sum of neutrino mass. In particular, we want to analyze the correlations among the Dirac CP-violating phase δ , the three mixing angle, the Jarlskog invariant J_{CP} , the effective neutrino mass m_{ee} .

As is pointed out in Ref.[14], the six textures compatible with the neutrino oscil-

lation data are given by

$$\begin{aligned}
(M_\nu)^I &= \begin{pmatrix} \Delta & 0 & \times \\ 0 & \times & \times \\ \times & \times & \times \end{pmatrix} & (M_\nu)^{II} &= \begin{pmatrix} \Delta & \times & 0 \\ \times & \times & \times \\ 0 & \times & \times \end{pmatrix} & (M_\nu)^{III} &= \begin{pmatrix} \times & 0 & \times \\ 0 & \Delta & \times \\ \times & \times & \times \end{pmatrix} \\
(M_\nu)^{IV} &= \begin{pmatrix} \times & \times & 0 \\ \times & \times & \times \\ 0 & \times & \Delta \end{pmatrix} & (M_\nu)^V &= \begin{pmatrix} \times & \Delta & \times \\ \Delta & 0 & \times \\ 0 & \times & \times \end{pmatrix} & (M_\nu)^{VI} &= \begin{pmatrix} \times & \times & \Delta \\ \times & \times & \times \\ \Delta & \times & 0 \end{pmatrix}
\end{aligned} \tag{1}$$

where the "0" stands for the zero element and the " Δ " stands for the zero cofactor.

In the basis where the charged mass matrix is diagonal, the neutrino mass texture M_ν under flavor basis is given by

$$M_\nu = V M_{diag} V^T \tag{2}$$

where M_{diag} is the diagonal matrix of neutrino mass eigenvalues $M_{diag} = \text{diag}(m_1, m_2, m_3)$. The Pontecorvo-Maki-Nakagawa-Sakata matrix[18] $V = U \cdot P$ can be parameterized as

$$V = UP = \begin{pmatrix} c_{12}c_{13} & c_{13}s_{12} & s_{13}e^{-i\delta} \\ -s_{12}c_{23} - c_{12}s_{13}s_{23}e^{i\delta} & c_{12}c_{23} - s_{12}s_{13}s_{23}e^{i\delta} & c_{13}s_{23} \\ s_{23}s_{12} - c_{12}c_{23}s_{13}e^{i\delta} & -c_{12}s_{23} - c_{23}s_{12}s_{13}e^{i\delta} & c_{13}c_{23} \end{pmatrix} \begin{pmatrix} 1 & 0 & 0 \\ 0 & e^{i\alpha} & 0 \\ 0 & 0 & e^{i(\beta+\delta)} \end{pmatrix} \tag{3}$$

where the abbreviation $s_{ij} = \sin \theta_{ij}$ and $c_{ij} = \cos \theta_{ij}$ is used. In neutrino oscillation experiments, CP violation effect is usually reflected by the Jarlskog rephasing invariant quantity[19] defined as

$$J_{CP} = s_{12}s_{23}s_{13}c_{12}c_{23}c_{13}^2 \sin \delta \tag{4}$$

Following the same step in Ref.[14], the texture zero and the zero minor in M_ν gives the mass ratio $(\frac{m_1}{m_2}, \frac{m_1}{m_3})$ and Majorana CP-violating phases (α, β) in terms of the $(\theta_{12}, \theta_{23}, \theta_{13}, \delta)$.i.e

$$\frac{m_1}{m_2} e^{-2i\beta} = - \frac{K_1 L_1 - K_2 L_2 + K_3 L_3 \pm (K_1^2 L_1^2 + (K_2 L_2 - K_3 L_3)^2 - 2K_1 L_1 (K_2 L_2 + K_3 L_3))^{\frac{1}{2}}}{2K_1 L_3} e^{2i\delta} \tag{5}$$

and

$$\frac{m_1}{m_3}e^{-2i\beta} = \frac{-K_1L_1 - K_2L_2 + K_3L_3 \pm (K_1^2L_1^2 + (K_2L_2 - K_3L_3)^2 - 2K_1L_1(K_2L_2 + K_3L_3))^{\frac{1}{2}}}{2K_1L_2} \quad (6)$$

where $K_1 = U_{x1}U_{y1}$, $K_2 = U_{x2}U_{y2}$, $K_3 = U_{x3}U_{y3}$ and

$$L_i = (U_{pj}U_{qj}U_{rk}U_{sk} - U_{tj}U_{uj}U_{vk}U_{wk}) + (j \leftrightarrow k) \quad (7)$$

with (i, j, k) a cyclic permutation of $(1, 2, 3)$. With the help of (5) and (6), the magnitudes of mass ratios are

$$\rho = \left| \frac{m_1}{m_3}e^{-2i\beta} \right|, \quad \sigma = \left| \frac{m_1}{m_2}e^{-2i\alpha} \right| \quad (8)$$

as well as the two Majorana CP-violating phases

$$\alpha = -\frac{1}{2}\arg\left(\frac{m_1}{m_2}e^{-2i\alpha}\right), \quad \beta = -\frac{1}{2}\arg\left(\frac{m_1}{m_3}e^{-2i\beta}\right) \quad (9)$$

The neutrino mass ratios ρ and σ are related to the ratios of two neutrino mass-squared ratios obtained from the solar and atmosphere oscillation experiments as

$$R_\nu \equiv \frac{\delta m^2}{|\Delta m^2|} = \frac{2\rho^2(1 - \sigma^2)}{|2\sigma^2 - \rho^2 - \rho^2\sigma^2|} \quad (10)$$

where $\delta m^2 \equiv m_2^2 - m_1^2$ and $\Delta m^2 \equiv m_3^2 - m_1^2$. For normal neutrino mass hierarchy(NH), the latest global-fit neutrino oscillation experimental data, at the 1σ , 2σ and 3σ confidential level, is list as follows[22]

$$\begin{aligned} \theta_{12} &= 33.6_{(-1.0, -2.0, -3.0)}^{o(+1.2, +2.2, +3.3)} \\ \theta_{23} &= 38.4_{(-1.2, -2.2, -3.2)}^{o(+1.6, +3.6, +14.6)} \\ \theta_{13} &= 8.9_{(-0.4, -0.9, -1.4)}^{o(+0.5, +0.9, +1.3)} \\ \delta m^2 &= 7.54_{(-0.22, -0.39, -0.55)}^{(+0.26, +0.46, +0.64)} \times 10^{-5} eV^2 \\ \Delta m^2 &= 2.43_{(-0.10, -0.16, -0.24)}^{(+0.06, +0.12, +0.19)} \times 10^{-3} eV^2 \end{aligned} \quad (11)$$

For the inverted neutrino mass hierarchy(NH), the differences compared with the NH are so slight that we shall use the same values given above. It is noted that the global analysis tends to give a θ_{23} less than 45° at 2σ and 1σ level. The Majorana nature of neutrino can be determined if any signal of neutrinoless double decay is observed,

implying the violation of leptonic number violation. The decay ratio is related to the effective of neutrino m_{ee} , which is written as

$$m_{ee} = |m_1 c_{12}^2 c_{13}^2 + m_2 s_{12}^2 c_{13}^2 e^{2i\alpha} + m_3 s_{13}^2 e^{2i\beta}| \quad (12)$$

Although a 3σ result of $m_{ee} = (0.11 - 0.56)$ eV is reported by the Heidelberg-Moscow Collaboration[23], this result is criticized in Ref [24] and shall be checked by the forthcoming experiment. It is believed that that the next generation $0\nu\beta\beta$ experiments, with the sensitivity of m_{ee} being up to 0.01 eV, will open the window to not only the absolute neutrino mass scale but also the Majorana-type CP violation. Besides the $0\nu\beta\beta$ experiments, a more severe constraint was set from the recent cosmology observation. Recently, an upper bound on the sum of neutrino mass $\sum m_i < 0.23$ eV is reported[5] by Plank Collaboration combined with the WMAP, high-resolution CMB and BAO experiments.

In the numerical analysis, We randomly vary the three mixing angles $(\theta_{12}, \theta_{23}, \theta_{13})$ in their 3σ range. Up to now, no bound was set on Dirac CP-violating phase δ at 3σ level, so we vary it randomly in the range of $[0, 2\pi]$. Using Eq. (10), the mass-squared difference ratio R_ν is determined. Then the input parameters is empirically acceptable when the R_ν falls inside the the 3σ range of experimental data, otherwise they are excluded. Finally, we get the value of neutrino mass and Majorana CP-violating α and β though Eq.(8), (9). Since we have already obtained the absolute neutrino mass $m_{1,2,3}$ and (α, β) , the further constraint from cosmology should be considered. In this work, we set the upper bound on the sum of neutrino mass $\sum m_i$ less than 0.23 eV.

In Fig.1-10, we demonstrate the correlations for all six pattern. The main results and the discussion are summarized as follows:

1) The Type-I and Type-II patterns are phenomenological acceptable only for inverted mass hierarchy, as mentioned in Ref.[14]. The type-I pattern are related to the type-II pattern by the $\mu - \tau$ symmetry[25], leading to the similar allowed resign for both patterns. One can see from the Fig.1 and Fig. 2 that in the light of a large θ_{13} the Dirac CP-violating phase δ can only acceptable at around $\pi/2(3\pi/2)$. The strong bound on δ is unusual and can be verified or excluded in future experiments.

The value of θ_{23} and θ_{12} are fully covered in 3σ level range. The m_{ee} for both type-I and type-II pattern lie in the range of $0.044\text{eV} < m_{ee} < 0.05\text{eV}$, which is in the scope of accuracy of $0\nu\beta\beta$ decay experiment near the future. For the maximal CP-violating $\delta = \pi/2$ or $\delta = 3\pi/2$, the $|J_{CP}| \geq 3\%$ is achieved, which is accessible to the future long-baseline neutrino oscillation experiments.

2) The allowed region of type-III patterns are shown in Fig.(3) for inverted hierarchy and Fig.(4) for normal hierarchy. For the IH pattern, θ_{23} lies below the maximality. Interestingly, the $\theta_{12} > 34^\circ$ and $\theta_{23} < 40^\circ$ are satisfied when the Dirac CP-violating phase δ falls into the region of $0^\circ \sim 50^\circ$ ($310^\circ \sim 360^\circ$), leading to $0.015\text{eV} < m_{ee} < 0.030\text{eV}$ and $|J_{CP}| < 0.03$. However, δ is also highly constrained at around $\pi/2$ ($3\pi/2$), where the full 3σ range of mixing angle are covered and $0.050\text{eV} < m_{ee} < 0.090\text{eV}$. The Jarlskog invariant J_{CP} is close to its maximum, i.e. $|J_{CP}| \geq 3\%$, which is promising to be explored in the next-generation long-baseline neutrino oscillation experiment. On the other hand, the Fig.(4) illustrates more complicated correlations for the NH pattern. There are unconstrained parameter space for δ , θ_{12} , θ_{13} and J_{CP} . However, we get a strongly constrained $\theta_{23} > \pi/4$ if δ lie in the range of $120^\circ \sim 240^\circ$ and $m_{ee} < 0.005\text{eV}$, rendering it very challenging to be detected in future $0\nu\beta\beta$ experiments.

3) We present the scatter plots of type-IV in Figure.(5) for IN case and Figure.(6) for NH case. For the inverted hierarchy, the Dirac CP-violating phase δ is limited to two regions, i.e. $120^\circ \sim 240^\circ$ and highly constrained points $\delta = \pi/2$ ($3\pi/2$). The θ_{23} are all above maximal and thus phenomenological ruled out at 2σ level. The range of m_{ee} is the same to that of type-III. This is not a coincidence but because the type-IV and type-III are related by the $\mu - \tau$ symmetry. Thus the θ_{23}^{IV} and δ^{IV} of type-IV are respectively equal to the $\frac{\pi}{4} - \theta_{23}^{III}$ and $\pi - \delta^{III}$ of type-III pattern. The same situation also appears in NH case.

4) The allowed region of type-V pattern are illustrated in Fig.(7) and Fig.(8). One can see from the figure that for the IH case, the Dirac CP-violating phase δ are phenomenological acceptable in the range of $0^\circ \sim 80^\circ$ ($280^\circ \sim 360^\circ$) and $90^\circ \sim 95^\circ$ ($265^\circ \sim 270^\circ$). Although covering the whole 3σ data, the θ_{23} are excluded at 2σ

level when the δ lies in the rang $50^\circ \sim 80^\circ (280^\circ \sim 310^\circ)$. We also get $0.015\text{eV} < m_{ee} < 0.040\text{eV}$ for $0^\circ < \delta < 80^\circ (280^\circ < \delta < 360^\circ)$ and $0.045\text{eV} < m_{ee} < 0.085\text{eV}$ for $90^\circ < \delta < 95^\circ (265^\circ \sim 270^\circ)$. No strong bound on J_{CP} are obtained. For the NH case, we have δ constrained in the range $0^\circ \sim 40^\circ (320^\circ \sim 360^\circ)$ with $\theta_{12} > 34^\circ$, $|J_{CP}| < 0.02$ and $90^\circ \sim 100^\circ (260^\circ \sim 270^\circ)$ with $|J_{CP}| \geq 0.03$. For both δ allowed region, the θ_{23} is below the maximality and $0.005\text{eV} < m_{ee} < 0.080\text{eV}$.

5) In Fig.(9) and Fig.(10), we present the allowed region for type-VI pattern. As the previous cases, the type-VI pattern relates with the type-V pattern via $\mu - \tau$ symmetry and therefore we have δ restricted to the range of $85^\circ \sim 90^\circ (100^\circ \sim 180^\circ)$ and $180^\circ \sim 260^\circ (270^\circ \sim 275^\circ)$. The effective mass of $0\nu\beta\beta$ decay is the same as the ones of type-V, i.e. $0.015\text{eV} < m_{ee} < 0.040\text{eV}$. Just like the IH case, the θ_{23} and δ of type-VI are equal to the $\pi/4 - \theta_{23}$ and $\delta + \pi$ of type-V. In this sense, although the δ covers the 180° which is at around the best-fit value of CP-violating phase from the neutrino oscillation experiments[22], the θ_{23} is up the maximality and thus ruled out by 2σ results.

In Table.1, we present some generic predictions of all viable textures at two value of δ . i.e. $\delta \simeq \pi/2$ where the Dirac CP symmetry is maximal violated and the best-fit point $\delta \simeq \pi$. One can see from the Table that the value of θ_{12} , θ_{23} and m_{ee} indicates important phenomenological implication for the model selection. We are particular interested in the type-III with the normal hierarchy and the type-VI with the inverted hierarchy. In both cases, two important feature emerges: (i) there leaves a space for $\theta_{23} < \pi/4$ indicated by the experimental data at 2σ level. (ii) the Dirac CP-violating phase δ is covered to its best-fit value: 1.09π [22]. Despite (i) and (ii) are not fully established yet, they are noteworthy in the model building[26] and deserve to be examined in future experiments.

In conclusion, the neutrino mass matrix with zero element and zero cofactor are stable against the running of GREs and can be realized by introducing discrete flavor symmetries with scalar singlets[14]. In this work, we carry out a numerical and comprehensive analysis of the viable textures with the current experimental data. We study the correlation between the Dirac CP-violating phase δ , three mixing angle and

the $0\nu\beta\beta$ effective mass m_{ee} . We examine the predictive powers of these correlations in the future experiments and demonstrate that they are essential in model selection. We present some notable predictions for all the survived textures at $\delta \simeq \pi/2$ and $\delta \simeq \pi$. Interestingly, the type-III(NH) and type-VI(IH) are found to be phenomenologically interesting by the fact that θ_{23} are possible located below $\pi/4$ and the Dirac CP-violating phase δ covers its best-fit value 1.09π . We expect that a cooperation between theoretical study from the flavor symmetry point view and a phenomenology study with updated experimental data will help us reveal the structure of neutrino mass texture.

Acknowledgments

The author would like to thank S. Dev, R.R. Gautam for the useful discussion during this work.

-
- [1] Q.R. Ahmad *et al.* (SNO Collaboration), Phys. Rev. Lett **89**, 011301(2002); K. Eguchi *et al.* (KamLAND Collaboration), Phys. Rev. Lett **90**, 021802(2003); M.H. Ahn *et al.* (K2K Collaboration), Phys. Rev. Lett **90**, 041801(2003).
 - [2] F.P. An *et al.* (DAYA-BAY Collaboration), Phys. Rev. Lett. **108**, 171803(2012).
 - [3] J.K. Ahn *et al.* (RENO Collaboration), Phys. Rev. **D108**, 191802(2012).
 - [4] G. Hinshaw *et al.* (WMAP Collaboration), arXiv: 1212.5226.
 - [5] P.A.R. Ade *et al.* (Planck Collaboration), arXiv: 1303.5076.
 - [6] S.M. Bilenky and C. Giunti, Mod. Phys. Lett. **A16**, 1230015(2012).
 - [7] H. Fritzsch, M. Gell-Mann, and P. Minkowski, Phys. Lett. **B59**, 256(1975); P. Minkowski, Phys. Lett. **B67**, 421(1977); T. Yanagida, in *Proceedings of Workshop on Unified Theory and the Baryon Number of the Universe*, edited by O. Sawada and A. Sugamoto(KEK, Tsukuba, 1979), p. 95; M. Gell-Mann, P. Ramond, and Slansky, in *Supergravity*, edited by P. van. Nieuwenhuizen and D.Z. Freeman (North-Holland,

- Amsterdam,1979), p. 315; R.N. Mohapatra and G. Senjanovic, Phys. Rev. Lett. **44**, 912(1980); J. Schechter and J. W. F. Valle, Phys. Rev. **D22**, 2227(1980); J. Schechter and J. W. F. Valle, Phys. Rev. **D25**, 774(1982).
- [8] P.H. Frampton, S. L. Glashow, and D. Marfatia, Phys. Lett. **B536**, 79(2002); Z.-z. Xing, Phys. Lett. **B530**, 159(2002); M. Randhawa, G. Ahuja, and M. Gupta, Phys. Lett. **B643**, 175(2006); A. Merle, and W. Rodejohann, Phys. Rev. **D73**, 073012(2006); S. Dev, S. Kumar, S. Verma, and S. Gupta, Phys. Rev. **D76**, 013002(2007); S. Dev, S. Kumar, S. Verma, and S. Gupta, Nucl. Phys. **B784**, 103(2007); G. Ahuja, S. Kumar, M. Randhawa, M. Gupta, and S. Dev, Phys. Rev. **D76**, 013006(2007); S. Dev, S. Kumar, Mod. Phys. Lett. **A22**, 1401(2007); S. Kumar, Phys. Rev. **D84**, 077301(2011); P.O. Ludl, S. Morisi, and E. Peinado, Nucl. Phys. **B857**, 411(2012); W. Grimus. and P.O. Ludl, arXiv:1208.4515; D. Meloni, and G. Blankenburg, Nucl. Phys. **B867**, 749(2013); H. Fritzsch, Z.-z. Xing, and S. Zhou, J. High Energy Phys. 09 (2011)083.
- [9] S. Kaneko, H. Sawanaka, and M. Tanimoto, J. High Energy Phys. 08 (2005)073; S. Dev, S. Verma, and S. Gupta, Phys. Lett. **B687**, 53(2010); S. Dev, S. Gupta, and R.R. Gautam, Phys. Rev. **D82**, 073015(2010); S. Goswami, S. Khan, and A. Watanabe, Phys. Lett. **B687**, 53(2010), W. Grimus, and P. O. Ludl, arXiv: 1208.4515.
- [10] J.-Y. Liu and S. Zhou, Phys. Rev. **D87**, 093010(2013).
- [11] X.-G. He and A. Zee, Phys. Rev. **D68**, 037302(2003).
- [12] G.C. Branco, R. Gonzalez Felipe, F.R. Joaquim, and T. Yanagida, Phys. Lett. **B562**, 265(2003); B.C. Chauhan, J. Pulido, and M. Picariello, Phys. Rev. **D73**, 053003(2006).
- [13] L. Lavoura, Phys. Lett. **B609**, 317(2005); E.I. Lashin and N. Chamoun, Phys. Rev. **D78**, 073002(2008); E.I. Lashin and N. Chamoun, Phys. Rev. **D80**, 093004(2009); S. Dev, S. Gupta, and R.R. Gautam, Mod. Phys. Lett. **A26**, 501(2011); S. Dev, S. Gupta, R.R. Gautam, and L. Singh, Phys. Lett. **B706**, 168(2011); T. Araki, J. Heeck, and J. Kubo, J. High Energy Phys. 07 (2012)083; S. Verma, Nucl. Phys. **B854**, 340(2012); S. Dev, R.R. Gautam, and L. Singh, arXiv: 1309.4219;
- [14] S. Dev, S. Verma, S. Gupta, and R.R. Gautam, Phys. Rev. **D81**, 053010(2010); J. Liao, D. Marfatia, K. Whisnant, arXiv: 1311.2639.

- [15] H.A. Alhendi, E.I. Lashin, and A.A. Mudlej, Phys. Rev. **D77**, 013009(2008).
- [16] S. Dev, R.R. Gautam, and L. Singh, Phys. Rev. **D87**, 073011(2013).
- [17] S. Dev, R.R. Gautam, and L. Singh, Phys. Rev. **D88**, 033008(2013); W. Wang, Eur. Phys. J. **C73**, 2551(2013).
- [18] B. Pontecorvo, Zh. Eksp. Teor. Fiz. **33**, 549(1957); Z. Maki, M. Nakagawa, and N. Sakata, Prog. Theor. Phys. **28**, 870(1962).
- [19] C. Jarlskog, Phys. Rev. Lett. **55**, 1039(1985).
- [22] G.L. Fogli, E. Lisi, A. Marrone, D. Montanino, A. Palazzo, and A.M. Rotunno, Phys. Rev. **D86**, 013012(2012); D. V. Forero, M. Tortola, and J. W. F. Valle, Phys. Rev. **D86**, 073012(2012); M. C. Gonzalez-Garcia, Michele Maltoni, Jordi Salvado, and Thomas Schwetz, J. High Energy Phys. 12 (2012)123.
- [23] H.V. Klapdor-Kleingrothaus, A. Dietz, H.L. Harney, and I.V. Krivosheina, Mod. Phys. Lett. **A16**, 2409(2001).
- [24] C.E. Aalseth *et al.* Mod. Phys. Lett. **A17**, 1475(2002); F. Feruglio, A. Strumia, and F. Vissani, Nucl. Phys. **B637**, 345(2002).
- [25] T. Fukuyama and H. Nishiura, arXiv: 9702253; R. N. Mohapatra and S. Nussinov, Phys. Rev. D60, 013002, (1999); E. Ma and M. Raidal, Phys. Rev. Lett. 87, 011802 (2001); C. S. Lam, Phys. Lett. B507, 214 (2001); K. R. S. Balaji, W. Grimus and T. Schwetz, Phys. Lett. B508, 301 (2001); W. Grimus and L. Lavoura, Acta Phys. Pol. B32, 3719 (2001).
- [26] L. Lavoura, W. Rodejohann, A. Watanabe, Phys. Lett. **B726**, 352(2013).

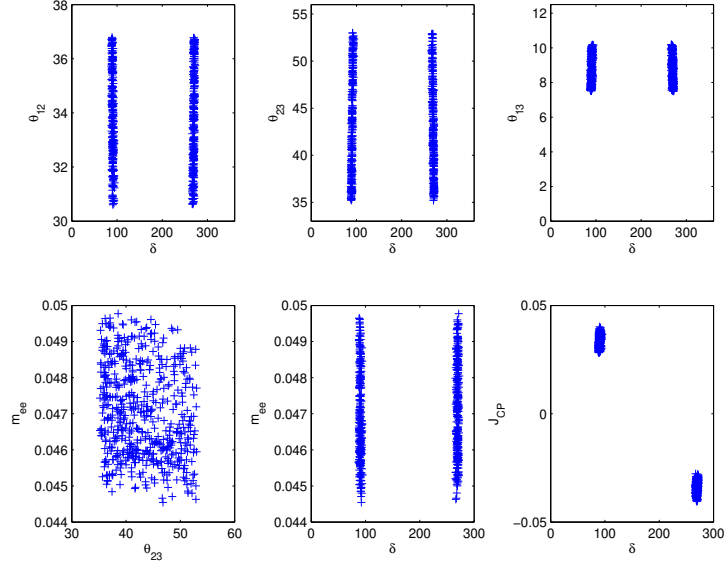


Figure 1: The plots for pattern type-I (IH).

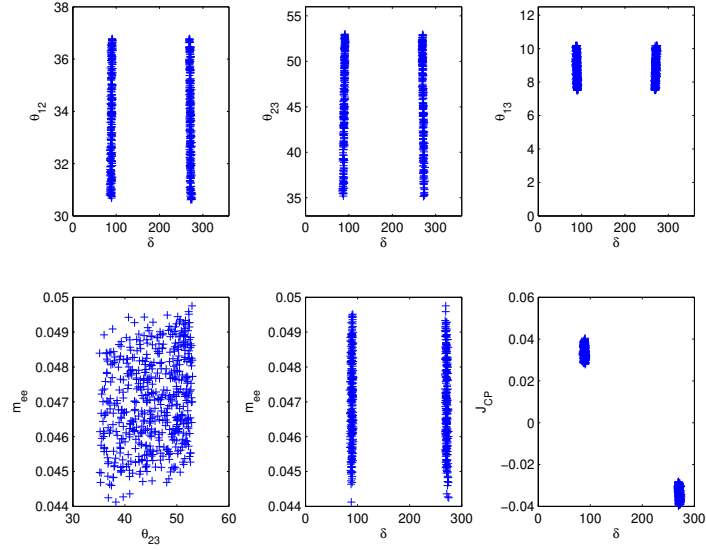


Figure 2: The plots for pattern type-II (IH).

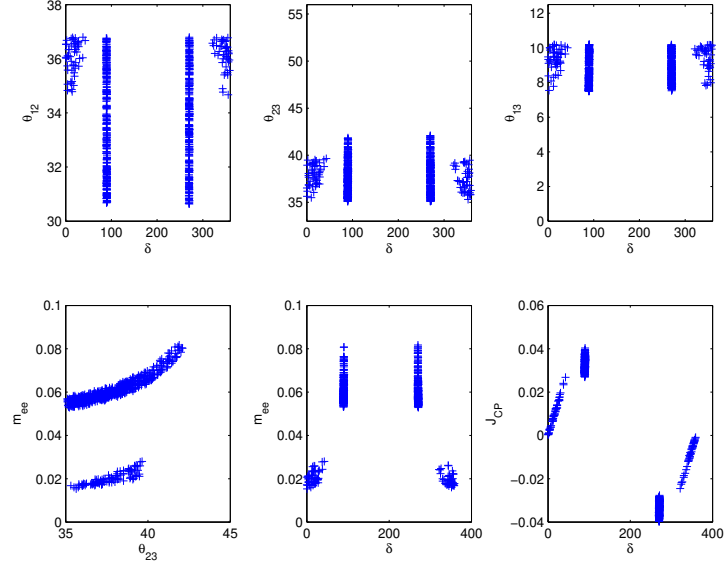


Figure 3: The plots for pattern type-III (IH).

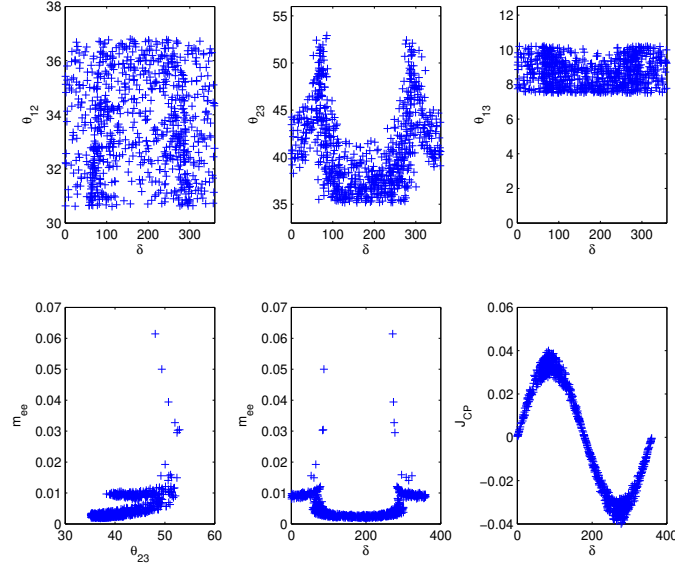


Figure 4: The plots for pattern type-III (NH).

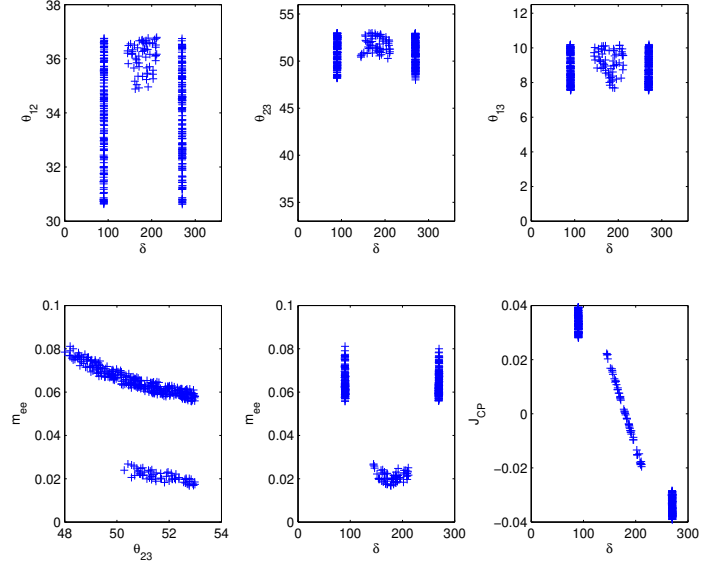


Figure 5: The plots for pattern type-IV (IH).

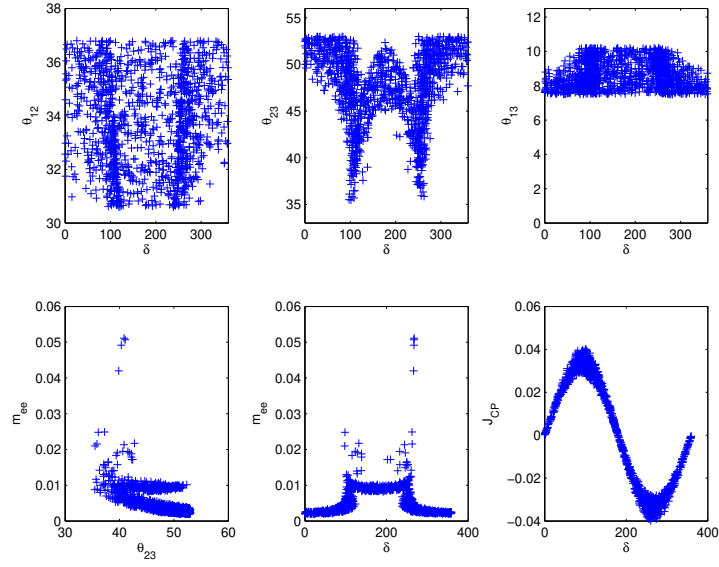


Figure 6: The plots for pattern type-IV (NH).

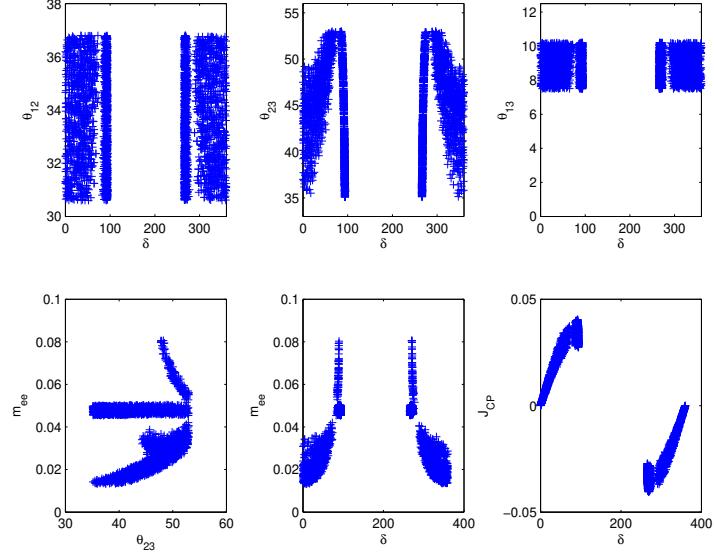


Figure 7: The plots for pattern type-V (IH).

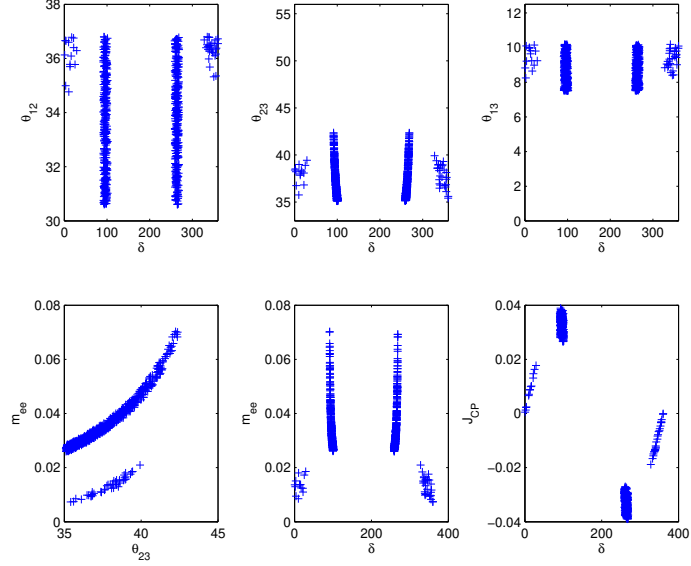


Figure 8: The plots for pattern type-V (NH).

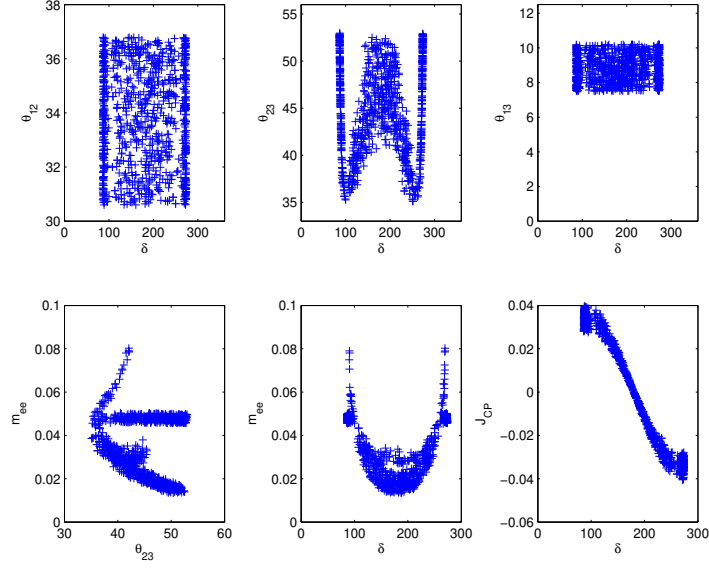


Figure 9: The plots for pattern type-VI (IH).

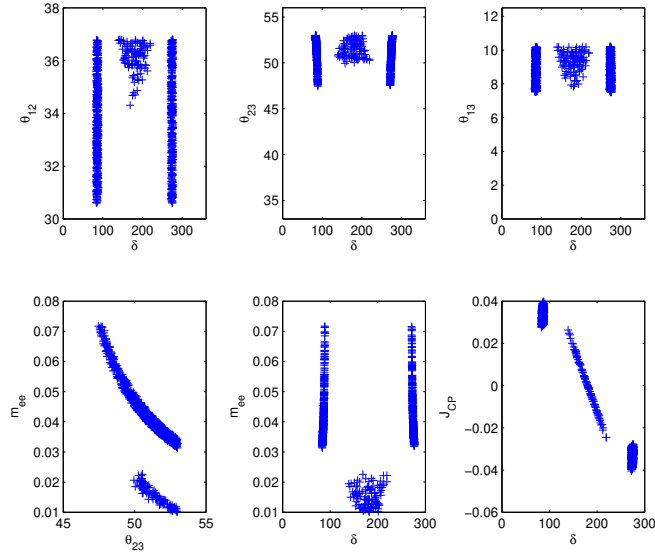


Figure 10: The plots for pattern type-VI (NH).

Table I: Some generic predictions for the viable textures at $\delta \approx \pi/2$ and $\delta \approx \pi$.

Texture	$\delta \approx \pi/2$	$\delta \approx \pi$
type-I(IH)	$0.044\text{eV} < m_{ee} < 0.050\text{eV}$	not allowed
type-II(IH)	$0.044\text{eV} < m_{ee} < 0.050\text{eV}$	not allowed
type-III(IH)	$\theta_{23} < \pi/4, 0.050\text{eV} < m_{ee} < 0.090\text{eV}$	not allowed
type-III(NH)	$0.002\text{eV} < m_{ee} < 0.030\text{eV}$	$\theta_{23} < \pi/4, m_{ee} < 0.007\text{eV}$
type-IV(IH)	$\theta_{23} > 47^\circ, 0.050\text{eV} < m_{ee} < 0.090\text{eV}$	$\theta_{12} > 34^\circ, \theta_{23} > 48^\circ, 0.015\text{eV} < m_{ee} < 0.030\text{eV}$
type-IV(NH)	$0.002\text{eV} < m_{ee} < 0.030\text{eV}$	$\theta_{23} > \pi/4, 0.007\text{eV} < m_{ee} < 0.014\text{eV}$
type-V(IH)	$0.040\text{eV} < m_{ee} < 0.080\text{eV}$	not allowed
type-V(NH)	$38^\circ < \theta_{23} < 43^\circ, 0.025\text{eV} < m_{ee} < 0.075\text{eV}$	not allowed
type-VI(IH)	$\theta_{23} > 42^\circ, 0.050\text{eV} < m_{ee} < 0.080\text{eV}$	$\theta_{23} > 40^\circ, 0.010\text{eV} < m_{ee} < 0.035\text{eV}$
type-VI(NH)	$\theta_{23} > 47^\circ, 0.030\text{eV} < m_{ee} < 0.075\text{eV}$	$\theta_{12} > 34^\circ, \theta_{23} > 49^\circ, 0.010\text{eV} < m_{ee} < 0.025\text{eV}$